ORNL/CP-99043

CONF-980504--

THE EFFECT OF MICROSTRUCTURE AND TEMPERATURE ON THE OXIDATION BEHAVIOR OF TWO-PHASE Cr-Cr_2X (X=Nb,Ta) ALLOYS

M.P. Brady and P.F. Tortorelli
Metals and Ceramics Division
Oak Ridge National Laboratory
Oak Ridge, TN, USA 37831-6115

The oxidation behavior of Cr(X) solid solution (Cr_{ss}) and Cr_2X Laves phases (X=Nb,Ta) was studied individually and in combination at 950-1100°C in air. The Cr_{ss} phase was significantly more oxidation resistant than the Cr_2X Laves phase. At 950°C, two-phase alloys of Cr-Cr_2Nb and Cr-Cr_2Ta exhibited "in-situ" internal oxidation, in which remnants of the Cr_2X Laves phase were incorporated into a growing chromia scale. At 1100°C, the Cr-Cr_2Nb alloys continued to exhibit in-situ internal oxidation, which resulted in extensive O/N penetration into the alloy ahead of the alloy-scale interface and catastrophic failure during cyclic oxidation. In contrast, the Cr-Cr_2Ta alloys exhibited a transition to selective Cr oxidation and the formation of a continuous chromia scale. The oxidation mechanism is interpreted in terms of multiphase oxidation theory.

INTRODUCTION

Two-phase Cr(X)-Cr_2X alloys (X=Nb,Ta) are under development for high temperature (>1000°C) structural applications in advanced fossil energy conversion and combustion systems [1]. The microstructure of these alloys consists of Cr_2X Laves phase particles dispersed in a Cr(X) solid solution (Cr_{ss}) matrix. The Cr_2X Laves phase particles provide high temperature strength, and the Cr_{ss} phase is a potential source of ductility and oxidation resistance. Preliminary evaluation of current Cr-(6-10)Ta (atomic percent, at.%) based alloys (with proprietary alloying additions) indicate a 1200°C tensile fracture strength of 350 MPa, room temperature fracture toughness in the 10-12 MPa$\sqrt{m}$ range, and high temperature oxidation resistance in the range of commercial chromia-forming alloys [1]. The goal of the present work is to develop a mechanistic understanding of the oxidation of binary, two-phase Cr_{ss}-Cr_2Nb (Cr-Cr_2Nb for short) and Cr-Cr_2Ta alloys in support of the alloy development effort. To accomplish this, the oxidation behavior of Cr_{ss} and Cr_2X Laves phases was studied individually and in combination at 950-1100°C in air.

DISCLAIMER

EXPERIMENTAL

Small 50-60 g castings of Cr-Cr_2X based alloys were prepared by arc melting and drop casting in a chilled copper mold. Six alloys were chosen for study (all compositions are reported in atomic percent, at.%): Cr-1Nb and Cr-1Ta to represent the Cr_{ss} phase, Cr-31Nb and Cr-31Ta to represent the Cr_2X Laves phase, and hypoeutectic two-phase Cr-6Nb and Cr-8Ta alloys, selected based on mechanical property development considerations. The Cr-Ta alloys are plotted on the binary Cr-Ta phase diagram [2,3] shown in Fig. 1. The binary Cr-Nb phase diagram (not shown) is similar to the Cr-Ta diagram except that the Cr_{ss} + Cr_2X eutectic falls at 18.5 at.% Nb [4], as opposed to about 9-10 at.% Ta [3].

The chemical analyses of the alloys are reported in Table I. The Cr source used to make the alloys (except for Cr-6Nb) was found to be impure, and contained large quantities of oxygen and sulfur. To examine the effects of the these impurities, additional Cr-1Nb and Cr-1Ta alloys were cast with a high purity electrolytic Cr provided by JMC (USA).

Table I- Alloy compositions measured by inductively coupled plasma spectroscopy and combustion techniques.

Alloy	Nb (at.%)	Ta (at.%)	Impurities (weight parts per million)			
			O	N	C	S
Cr-1Nb	0.78	-	6890	50	200	360
*Cr-1Nb	1.03	-	99	<3	<100	<10
Cr-6Nb	6.17	-	410	60	200	110
Cr-31Nb	30.69	-	3780	50	100	200
Cr-1Ta	-	0.38	7030	55	100	320
*Cr-1Ta	-	1.00	148	<3	<100	<10
Cr-8Ta	-	7.92	2501	19	<100	70
Cr-31Ta	-	31.05	2886	30	200	120
Cr	-	-	7058	112	200	350
JMC Cr	-	-	170	20	<100	<10

- Not Present

* Made with JMC Cr

The alloy castings were heat treated for 24 h at 1300°C in vacuum. Oxidation coupons were polished to a 600-grit finish by standard metallographic techniques. Oxidation behavior was studied by thermogravimetric analysis (TGA) for 1 week (168 h) at 950°C in filtered compressed dry air and for 24 h at 950°C in a tube furnace open to "room" air of varying daily humidity. Little chromia volatility was observed at this

temperature. No difference in oxidation behavior in dry or room air was detected for the alloys under the time/temperature conditions studied. Some scatter in the TGA data (168h total weight changes ranged from 3-7 mg/cm^2) was observed from run to run for the low and high purity Cr-1X alloys; however, there were no discernible trends. Consequently, only the TGA data for the high purity Cr-1X alloys are reported here.

The cyclic oxidation behavior of Cr-6Nb, Cr-8Ta, and as-cast Cr-10Nb and Cr-10Ta (made from the low purity Cr) was studied at 1100°C in a tube furnace open to room air. The Cr-10Nb alloy is hypoeutectic, while the Cr-10Ta alloy is slightly hypereutectic (Fig. 1). The samples were placed in a covered alumina crucible and inserted/removed from the furnace at temperature after intervals of 1, 4, 10, 30, 48, and 120 h of cumulative exposure. Significant chromia volatilization occurred as evidenced by green stains on the underside of the alumina crucible lid.

Oxidized coupons were characterized by x-ray diffraction (XRD), optical microscopy, and secondary mode scanning electron microscopy (SEM). Qualitative analysis of alloy and oxide phase composition was made by energy dispersive x-ray analysis (EDS). Room temperature Vicker's microhardness measurements (25-100g, 15s) were used to qualitatively evaluate the hardening associated with oxygen/nitrogen penetration into the alloy ahead of the alloy-scale interface.

RESULTS

At 950°C in air, the gravimetric kinetics for the Cr-Nb and Cr-Ta alloys were similar, with the Cr-31X Laves phase alloys much less oxidation resistant than the Cr_{ss} (Cr-1X) and two-phase Cr_{ss} + Laves phase Cr-6Nb and Cr-8Ta alloys (Fig. 2). The oxidation rates of the Cr_{ss} and two-phase alloys fell within the wide scatter band reported for chromia-forming alloys [5]. The Cr-Ta alloys tended to suffer from isothermal scale cracking, as evidenced by discontinuities in the gravimetric curves. All of the alloys except Cr-31Ta and Cr-31Nb suffered from extensive spallation on cooling.

After 24h at 950°C in air, the Laves alloy Cr-31Ta formed a continuous chromia scale (Fig. 3a). Energy dispersive x-ray analysis indicated that the metal underlying the chromia scale was enriched in Ta. After 168 h at 950°C, a thick, nonprotective, highly layered scale consisting of alternating chromia/Ta-rich layers was formed (Fig. 3b). In the scale region near the alloy-scale interface, EDS analysis suggested that the Ta-rich layers were metallic rather than oxide. The chromia/Ta-rich layer spacing near the scale-gas interface was too fine to analyze by EDS, and it was not determined whether the Ta-rich regions were metal or oxide. A similar layered scale was formed by the Cr-31Nb Laves alloy after both 24 and 168 h at 950°C in air. Shorter term exposures are needed to determine if Cr-31Nb was initially a continuous chromia scale former as was observed for Cr-31Ta.

SEM micrographs of Cr-8Ta after 24 h at 950°C in air and Cr-6Nb after 168 h at 950°C in air are shown in Fig. 4. Both scales consisted of an outer continuous layer of chromia, and an inner layer of chromia containing metallic Laves phase remnants of similar morphology, volume fraction, and distribution to the underlying alloy microstructure. EDS analysis of the Laves phase remnants in the scale indicated that they were depleted in Cr and possibly enriched in oxygen relative to the bulk Laves phase regions. Whether the remnants were still Laves phase, or the Ta_{ss} (or Nb_{ss}) phase with Cr in solution, was not determined.

Cyclic oxidation at 1100°C in air revealed significant differences between as-cast Cr-10Nb and Cr-10Ta (Fig. 5). The Cr-10Nb alloy suffered from extensive spallation and catastrophic failure. However, the Cr-10Ta alloy exhibited positive weight gains and no spallation throughout the 6-cycle, 120 h exposure. Similar trends were observed for Cr-6Nb and Cr-8Ta, with catastrophic failure of Cr-6Nb and positive weight gains of Cr-8Ta (slight scale spallation was observed on the final cycle). As noted in the experimental section, chromia volatility was significant at this temperature.

Figure 6 shows representative SEM cross-section micrographs of Cr-10Nb after 120 h (6 cycles) at 1100°C in air. All but 100-150 μm of the sample (original thickness of 1 mm) was consumed. The scale consisted of mixed Cr and Nb oxides. Extensive penetration of O/N ahead of the alloy-scale interface was evident. Microhardness indentation indicated that this zone was hardened and embrittled. Remnants of the alloy microstructure were retained in the external scale and the O/N affected zone.

In contrast to Cr-10Nb, a continuous chromia scale was formed on Cr-10Ta after 120 h (6 cycles) at 1100°C in air (Fig. 7). At the alloy-scale interface, a region with an increased volume fraction of the Cr_2Ta Laves phase and a decreased volume fraction of the Cr_{ss} phase was evident (phase identification by EDS only). Qualitatively, the relative volume fractions of Cr_{ss} and Cr_2Ta phases appear to be reversed relative to the bulk alloy. There was no evidence of extensive O/N penetration and embrittlement ahead of the alloy-scale interface, although EDS data did suggest that the Cr_{ss} and Cr_2Ta Laves phases in the depletion region at the alloy-scale interface were oxygen-rich relative to the bulk alloy.

DISCUSSION

The Cr_2X Laves phase exhibited poor oxidation resistance at 950°C in air due to the formation of a thick, nonprotective layered scale (Fig. 3b). However, the Cr_2Ta Laves phase alloy, Cr-31Ta, (and likely the Cr-31Nb alloy as well) were initially continuous chromia scale formers (Fig. 3a). The breakdown of the chromia scale is postulated to result primarily from a combination of low Cr diffusivity and the narrow Cr_2X Laves

phase Cr solubility range (Fig. 1), which leads to Cr depletion and Ta (or Nb) enrichment underneath the scale. When this Ta (or Nb) rich layer is oxidized, chromia scale formation is disrupted by rapidly growing Ta (or Nb) rich oxidation products. On consumption of the Ta (or Nb) rich layer, the cycle repeats. The layered nature of the scale is attributed to this ratcheting back and forth from Cr depletion to form chromia resulting in Ta (or Nb) enrichment/oxidation.

The oxidation behavior of the two-phase Cr_{ss} + Cr_2X Laves phase alloys can be interpreted in terms of the multiphase oxidation classification outlined by Gesmundo and Gleeson [6]. At 950°C in air, the scale microstructures formed by Cr-6Nb and Cr-8Ta were similar. In both cases, metallic Laves phase remnants were incorporated into the inner regions of an otherwise continuous chromia scale (Fig.4). Further, the alloy microstructure directly beneath the scale was unchanged relative to the remainder of the alloy. This morphology is qualitatively similar to the "in-situ" or diffusionless classification of internal oxidation [6].

In-situ internal oxidation is ideally observed under conditions of low oxidant pressures in binary two-phase alloys (such that the noble alloy component cannot oxidize) when the solubility and diffusivity of the reactive alloy component in the second phase is low [6]. The microstructure of the corroded region then closely follows that of the original alloy, and the resultant oxide scale incorporates second phase alloy particles of similar volume fraction, morphology, and distribution as was present in the alloy. The oxidation is referred to as in-situ or diffusionless since it occurs without appreciable diffusion of the less-noble alloy component. This situation is schematically outlined in Fig. 8.

The present Cr-Cr_2X alloy oxidation situation is much more complex than the ideal in-situ oxidation case. First, oxidation was conducted in air at atmospheric pressure. Second, the stability of Cr, Ta, and Nb in oxygen are thermodynamically similar. Third, the Cr_2X phase is a compound of limited solubility range situated in the middle of the phase diagram, not a terminal solid solution phase. Despite these complications, the mode of oxidation of the two-phase Cr-Cr_2X alloys at 950°C in air was strikingly similar to the ideal in-situ internal oxidation case described by Gesmundo and Gleeson (Fig. 4 vs Fig. 8).

A possible mechanistic route to the in-situ morphology of two-phase oxidation in the Cr-Cr_2X alloys would arise if Cr diffusivity in the Cr_2X Laves phase was sufficiently low that consumption of Cr to form chromia resulted in a transformation of the Cr_2X Laves phase to the Ta_{ss} (or Nb_{ss}) phase (refer to Fig. 1). The Ta_{ss} and Nb_{ss} phases would be expected to have a much higher solubility for oxygen/nitrogen than the Cr_{ss} phase, and so would saturate with oxygen/nitrogen while the Cr_{ss} phase was converted to oxide. (Alternatively, it is also possible that the metallic phase in the scale remained in the

Laves phase field, but that Cr depletion resulted in an increase in oxygen/nitrogen solubility). The EDS analysis of the Laves phase remnants in the scale formed on Cr-6Nb and Cr-8Ta is consistent with this supposition in that Cr depletion and oxygen enrichment were detected. (Wavelength dispersive measurements, which are needed to measure nitrogen, have not yet been performed). This speculated mechanism is also consistent with the absence of Laves remnants in the chromia scale near the scale-gas interface, which may have formed in part from outward diffusion of Cr from the Cr_2X Laves phase during the initial stages of oxidation. Quantitative compositional analysis of the phases in and near the scale needed to support this speculation are planned.

At 1100°C, the Cr-Cr_2Nb alloys (Cr-6Nb and Cr-10Nb) continued to exhibit in-situ oxidation (Fig. 6). This resulted in the formation of a nonprotective mixed Cr and Nb scale which mimicked the original structure of the alloy. It also resulted in extensive O/N penetration into the alloy ahead of the alloy-scale interface, which both hardened and embrittled the alloy. In contrast, the Cr-Cr_2Ta alloys (Cr-8Ta and Cr-10Ta) exhibited selective oxidation of Cr and the formation of a continuous chromia scale. According to Gesmundo and Gleeson [6], the ideal selective oxidation of a binary two-phase alloy would result in a zone underlying the scale which would be depleted in the reactive alloy component phase; in this case the Cr_{ss} phase. A Cr-depleted zone was observed underneath the chromia scale in Cr-10Ta. However it was two-phase and consisted of Cr_{ss} particles in a Cr_2Ta Laves matrix. Interestingly, this microstructure is the inverse of the bulk alloy microstructure, which consisted of Cr_2Ta Laves phase particles dispersed in a Cr_{ss} matrix.

Because the microstructure of the depletion zone remained in the Cr_{ss} + Cr_2Ta Laves binary two-phase field, there was no activity gradient to drive diffusion of Cr. However, outward diffusion of Cr from the alloy to form the chromia scale clearly did occur. This suggests that either the Cr_{ss} and Cr_2Ta phase compositions in this zone are not the equilibrium compositions (nonequilibrium process), or an extra degree of freedom was obtained by the dissolution of O or N into the alloy. The EDS analysis suggested the latter situation may be the case. However, further work is needed to confirm this supposition.

A key question for future work is why the Cr-Cr_2Ta alloys exhibited selective Cr oxidation while the Cr-Cr_2Nb alloys did not. A full understanding of this phenomenon is critical to the alloy development effort because the selective Cr oxidation route appears to minimize or even completely bypass the penetration of O/N into the alloy ahead of the alloy-scale interface (Fig. 6). Such O/N penetration leads to subsurface hardening and embrittlement. Preliminary results suggest that both microstructure and purity may be important, with fine eutectic Cr-Cr_2X mixtures and high levels of oxygen impurities (such that chromia inclusions are present) favoring the transition to selective Cr oxidation.

SUMMARY

1) At 950°C in air, the Cr_{ss} phase was significantly more oxidation resistant than the Cr_2X Laves phase.

2) At 950°C in air, hypoeutectic Cr-Cr_2Nb and Cr-Cr_2Ta two-phase alloys exhibited in-situ internal oxidation, in which remnants of the Cr_2X Laves phase were incorporated into a growing chromia scale.

3) At 1100°C in air, the hypoeutectic Cr-Cr_2Nb two-phase alloys continued to exhibit in-situ internal oxidation, which resulted in extensive O/N penetration into the alloy ahead of the alloy-scale interface and catastrophic failure during cyclic oxidation. In contrast, both hypoeutectic (Cr-8Ta) and hypereutectic (Cr-10Ta) Cr-Cr_2Ta two-phase alloys exhibited a transition to selective Cr oxidation and the formation of a continuous chromia scale.

ACKNOWLEDGEMENTS

The authors thank Brian Gleeson and Yan Niu for many helpful discussions and Jim Distefano, Bruce Pint, Christoph Leyens, and Ian Wright for reviewing this manuscript. The authors also thank JMC (USA) for donating high purity chromium for arc-melting purposes. This research was sponsored by the Fossil Energy Advanced Research and Technology Development (AR&TD) Materials Program, U. S. Department of Energy, under contract DE-AC05-96OR22464 with Lockheed Martin Energy Research Corporation.

REFERENCES

1. M. P. Brady, J. H. Zhu, C. T. Liu, P. F. Tortorelli, J. L. Wright, and C. A. Carmichael, submitted to proceedings of the 12th Annual Conference on Fossil Energy Materials, U.S. Department of Energy (1998).
2. M. Venkatraman and J.P. Neumann, in Binary Alloy Phase Diagrams Vol. 1, T.B. Massalaski, J.L. Murray, L.H. Bennett, and H. Baker eds., ASM, p. 867 (1986).
3. J.H. Zhu and C.T. Liu, unpublished research (1997).
4. D.J. Thoma and J.H. Perepezko, Materials Science and Engineering, A156, p. 97 (1992).
5. H. Hindam and D.P. Whittle, Oxidation of Metals, Vol. 18, nos. 5/6, p. 245 (1982).
6. F. Gesmundo and B. Gleeson, Oxidation of Metals, Vol. 44, Nos. 1/2, p. 211 (1995).

Keywords: Laves phase, internal oxidation, chromia, two-phase alloy oxidation

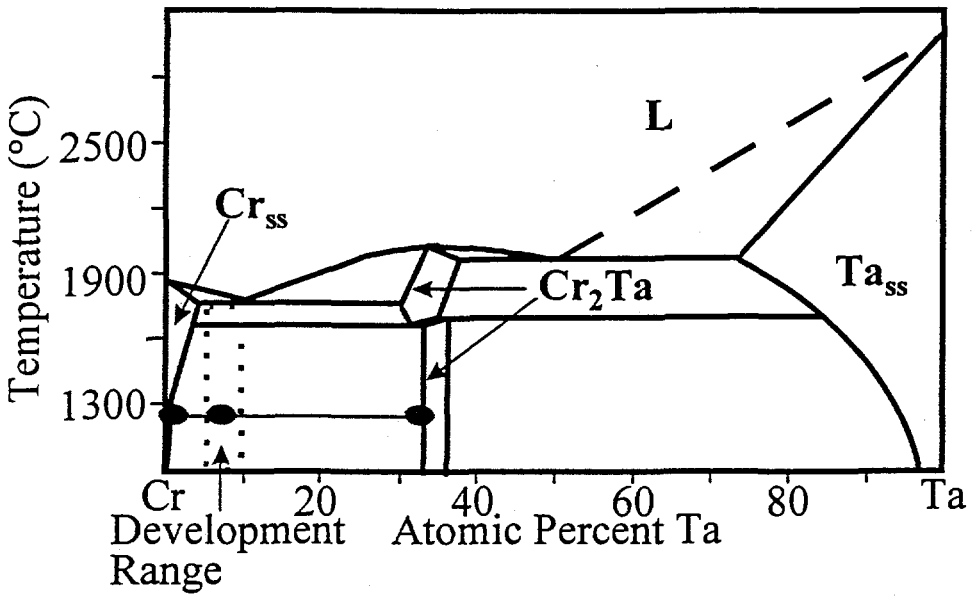

Fig. 1-Schematic binary Cr-Ta phase diagram [2,3].

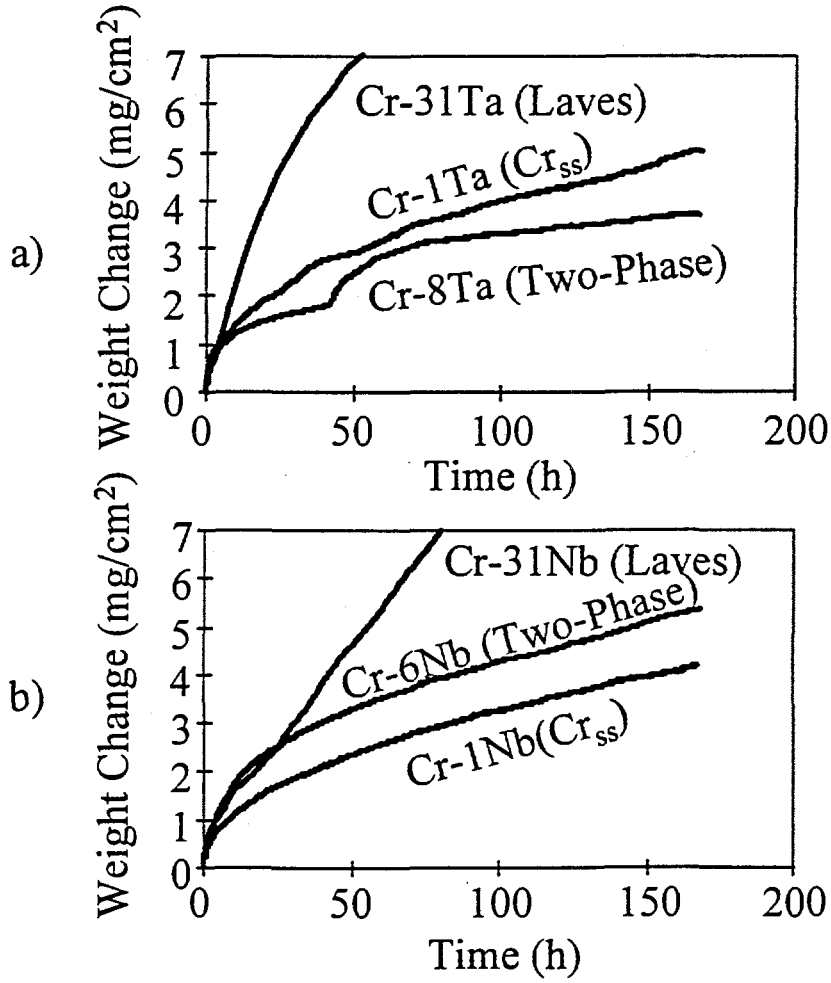

Fig. 2- TGA data at 950°C in filtered, compressed, dry air

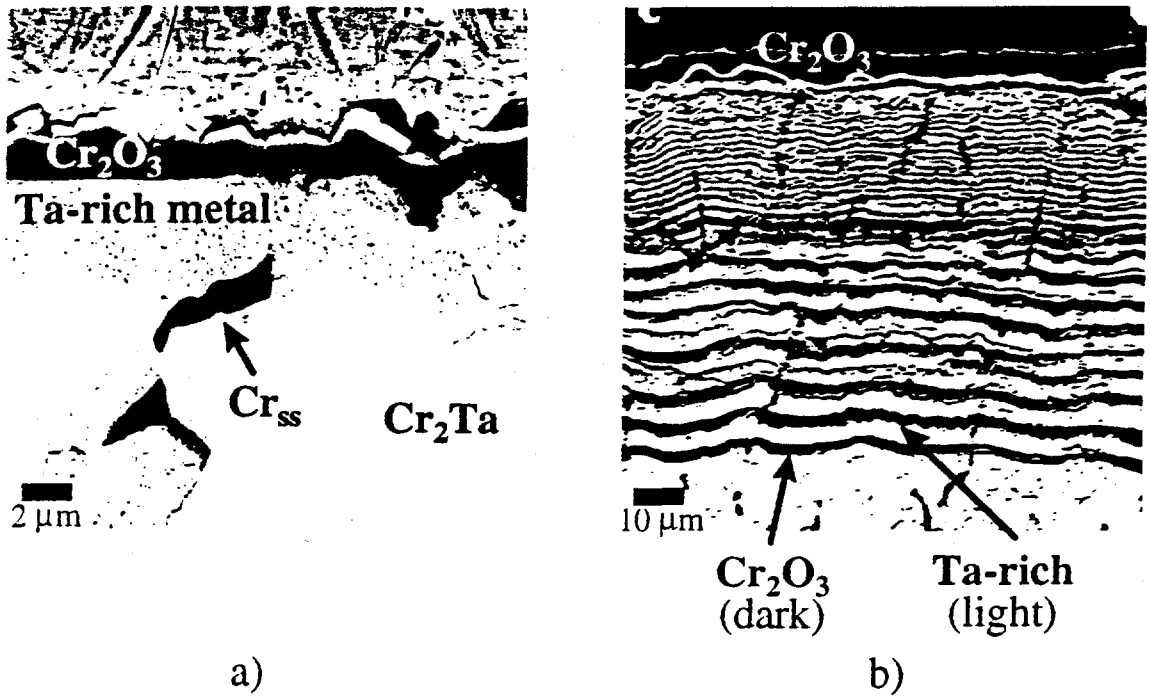

Fig. 3- SEM Cross-section micrographs of Cr-31Ta at 950°C in air. a) 24 h b) 168 h

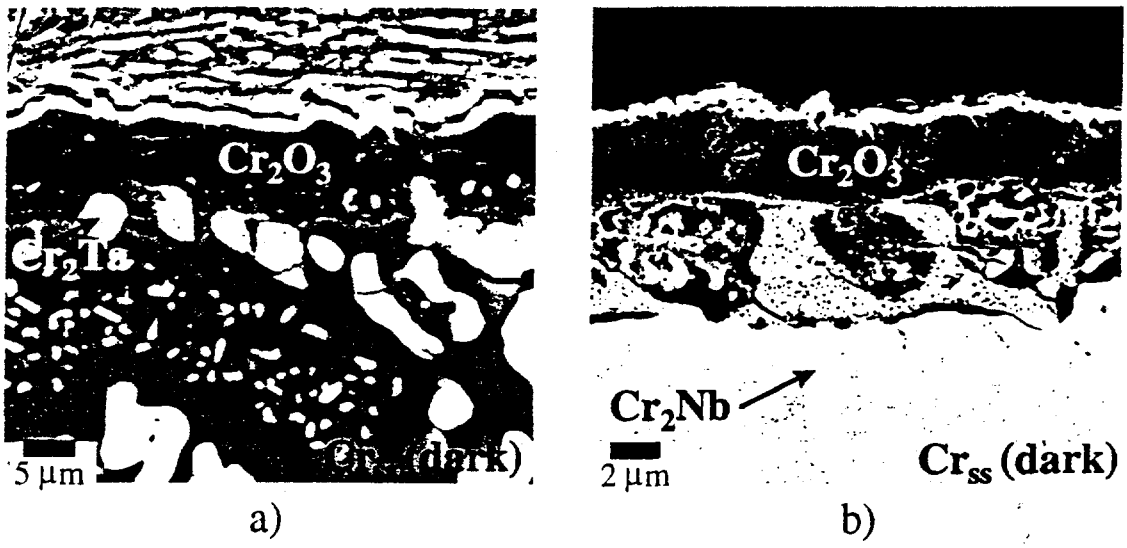

Fig. 4- SEM Cross-section micrographs after exposure at 950°C in air.
a) Cr-8Ta for 24 h b) Cr-6Nb for 168 h

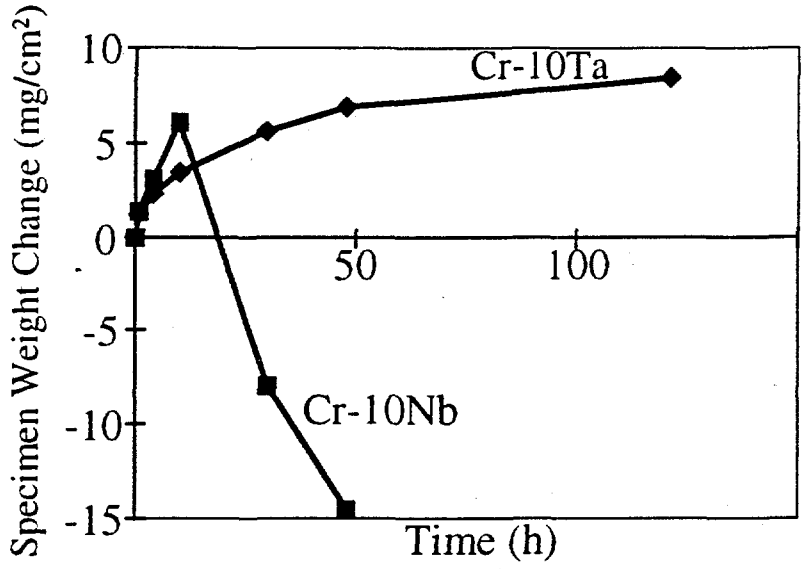

Fig. 5- Cyclic oxidation kinetics at 1100°C in air.

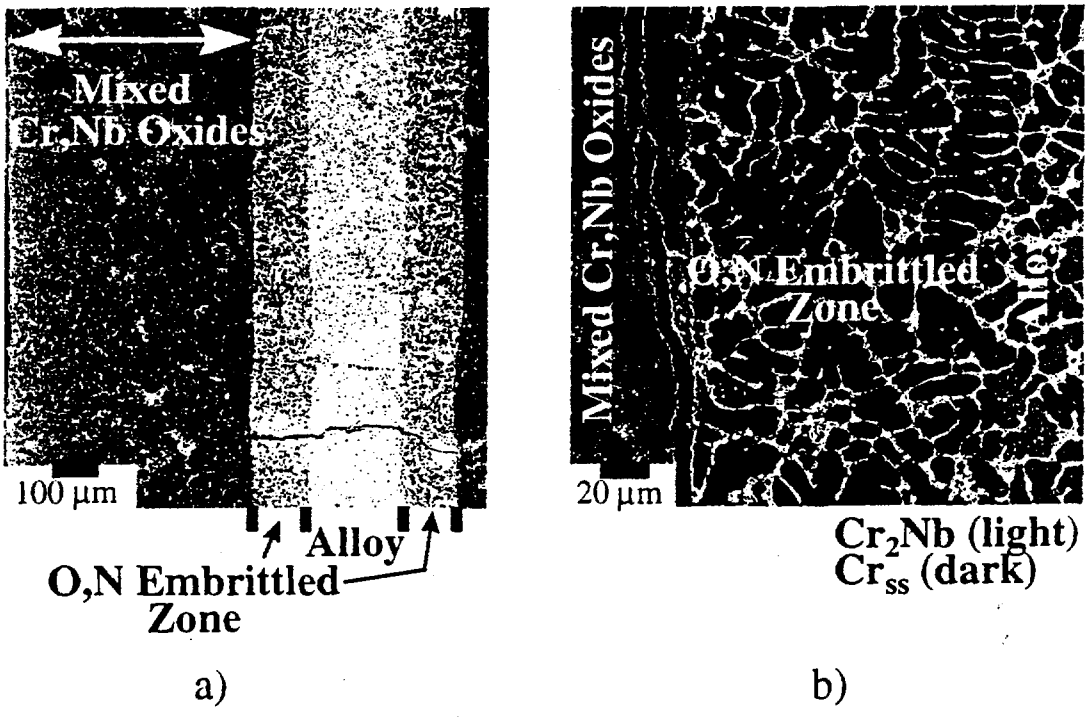

Fig. 6- SEM cross-section micrographs of Cr-10Nb after 120 h (6 cycles) at 1100°C in air. a) Low magnification overview b) Close-up of alloy/scale interface region

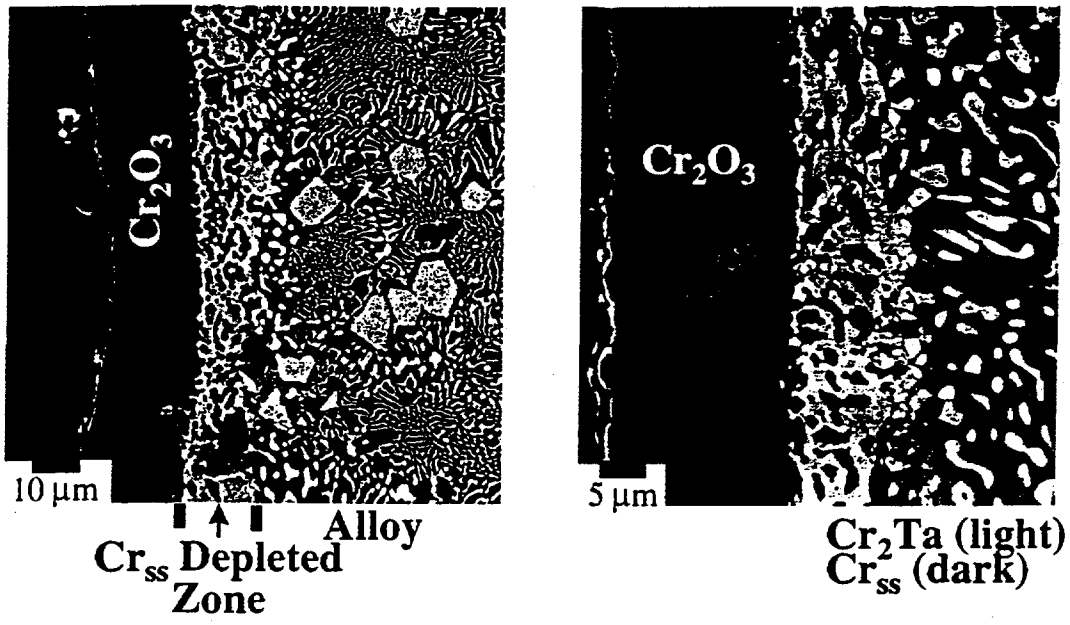

Fig. 7- SEM cross-section micrographs of Cr-10Ta after 120 h (6 cycles) at 1100°C in air.

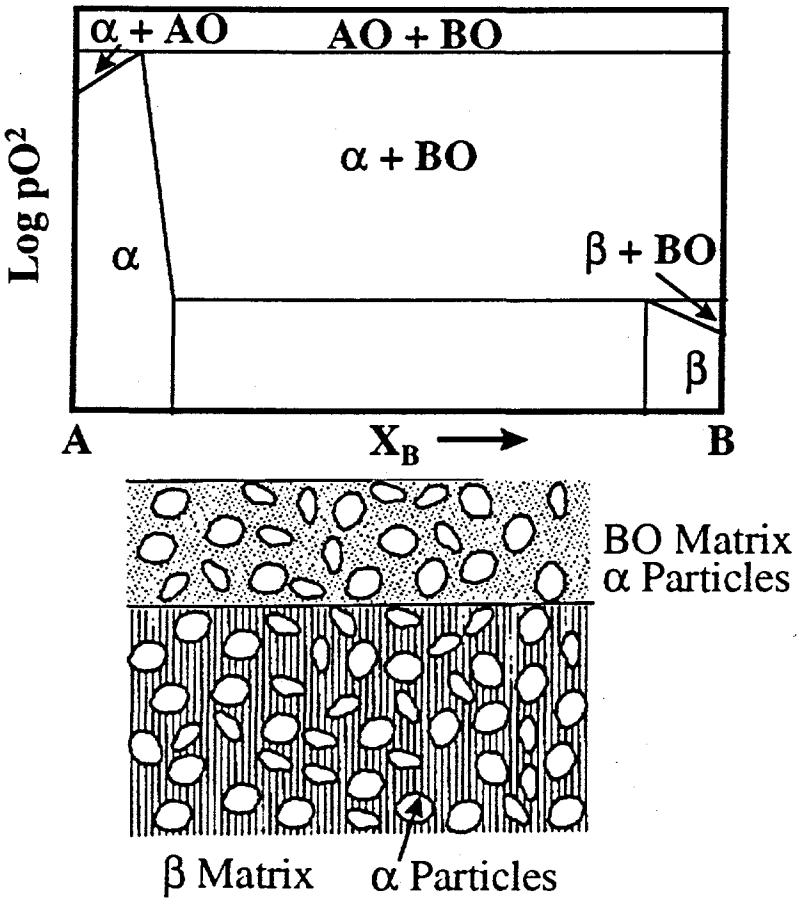

Fig. 8- Schematic ideal in-situ oxidation case (after Gesmundo and Gleeson [6]).